Sādhanā Vol. 40, Part 2, April 2015, pp. 307–333. © Indian Academy of Sciences

Tool position tracking control of a nonlinear uncertain flexible robot manipulator by using robust H_2/H_∞ controller via T–S fuzzy model

VAHID AZIMI[1,*], MOHAMMAD BAGHER MENHAJ[2] and AHMAD FAKHARIAN[3]

[1]Department of Electrical and Computer Engineering, Cleveland State University, Cleveland, OH, USA
[2]Department of Electrical Engineering, Amirkabir University of Technology, Tehran, Iran
[3]Department of Electrical, Biomedical and Mechatronic Engineering, Qazvin Branch, Islamic Azad University, Qazvin, Iran
e-mail: v.azimi@csuohio.edu; vahid.azimii@gmail.com

MS received 15 September 2013; revised 29 July 2014; accepted 12 December 2014

Abstract. In this paper, a robust H_2/H_∞ control with regional Pole-Placement is considered for tool position control of a nonlinear uncertain flexible robot manipulator. The uncertain nonlinear system is first approximated by Takagi and Sugeno's (T–S) fuzzy model. To achieve a better tracking, an extra state (error of tracking) is then augmented to the T–S model. Based on each local linear subsystem with augmented state, a regional pole-placement state feedback H_2/H_∞ controller is properly designed via linear matrix inequality (LMI) approach. Parallel Distributed Compensation (PDC) is also used to establish the whole controller for the overall system and the total linear system is obtained by using the weighted sum of the local linear systems. A fuzzy weighted online computation (FWOC) component is employed to update fuzzy weights in real time for different operating points of the system. Simulation results are presented to validate the effectiveness of the proposed controller like robustness and good load disturbance attenuation and accurate tracking, even in the presence of parameter variations and also load disturbances on the motor and the tool. The superiority of the proposed control scheme is finally highlighted in comparison with the Quantitative feedback theory (QFT) controller, the QFT controller of order 13, a polynomial controller and the so-called linear sliding-mode controller methods.

Keywords. Robust H_2/H_∞ control; T–S fuzzy model; LMI; PDC; FWOC component; flexible robot manipulator.

*For correspondence

1. Introduction

Robot manipulators have become progressively important in the field of flexible automation and manufacturing system in industrial applications such as material handling. Since the dynamics of robot manipulators are highly nonlinear and may contain uncertain parameters such as friction, many efforts have been made in developing control designs to achieve the accurate tracking control of robot manipulators (Zouand *et al* 2010; Islam & Liu 2011; Wai *et al* 2010). In this paper, control of a flexible manipulator benchmark system is investigated. In recent years, there has been an increasing interest in controlling robots and especially many researches of this benchmark problem should be appropriately considered as listed below. Moberg *et al* (2009) investigated a benchmark problem for robust feedback control of a flexible manipulator. Ohr *et al* (2006) presented identification of flexibility parameters of 6-axis industrial manipulator models. Wernholt & Gunnarsson 2006 proposed detection and estimation of nonlinear distortions in industrial robots. Moreover, other different papers and thesis of flexible manipulators have been published by Moberg (Moberg & Öhr 2005, 2008; Moberg *et al* 2008; Moberg 2007; Moberg & Hanssen 2007).

The dynamics of robot manipulators are highly nonlinear and change rapidly as the robot links move fast within its working range and may also contain uncertain parameters such as frictions. Generally, in a manipulator the control signal is motor torque and the main objective is tool position. The aim of robot manipulator control is position tracking of the tool when moving the tool along a certain desired path. Furthermore, control performance of robot manipulator in various applications is highly sensitive to variations of disturbance torque acting on the motor and tool and system parameters. Although aforementioned disturbances are troublous factors in the manipulator control system, in this paper an innovative robust position control will be presented to reduce their effects.

The main contribution of this research is robust H_2/H_∞ control of a nonlinear uncertain flexible robot manipulator. In this paper, the problem of robust H_2/H_∞ control of a robot manipulator which possesses not only parameter uncertainties but also external disturbances is considered. Recent researches show that a Takagi and Sugeon's fuzzy model (T–S) can be utilized to approximate global behavior of highly complex nonlinear systems. The large numbers of published papers have used the T–S fuzzy model technique for different drive systems (Chen & Wu 2010; Wai & Yang 2008; Azimi *et al* 2012a, b, c; Fakharian & Azimi 2012; Asemani & Majd 2013; Yang *et al* 2014a; Hu *et al* 2013). In the proposed method, a Takagi–Sugeno (T–S) fuzzy model is first designed on behalf of the underlying nonlinear plant. The fuzzy model is described by fuzzy IF-THEN rules which represent local input–output relations of the nonlinear system. In this research, tracking of tool position and minimization of motor torque are selected as the main objectives. In order to obtain an accurate tracking of tool position, an extra state is then augmented to the T–S fuzzy model. Afterward, for each fuzzy linear subsystem a robust H_2/H_∞ state feedback controller is designed with regional pole-placement based on Linear Matrix Inequality (LMI) formulation. In addition, several robust control schemes for different systems have been reported previously (Shayeghi *et al* 2008; Yue & Lam 2004; Li *et al* 2008; El-Mahallawy *et al* 2011; Azimi *et al* 2011, 2013a; Wu *et al* 2014; Yang *et al* 2014b; Kamal *et al* 2014). The Parallel Distributed Compensation technique (PDC) is utilized to design the controller for the overall system. On the other hand, the overall fuzzy model of the system is achieved by fuzzy "blending" of the local linear subsystem models. Furthermore, a Fuzzy Weighted Online Computation component (FWOC) is properly designed to update fuzzy weights in real time for different operating points of the system. Finally, simulation results show that the proposed method can effectively meet the performance requirements like robustness and good load disturbance rejection, good

tracking and fast transient responses of this manipulator. Our simulation records of robot manipulator via various existing control frameworks are also provided in this study to compare and display the superior performance of the proposed control scheme. To cut a long story short, if we want to render problem statement of this study, the major contributions can be highlighted as follows:

- Successful employment of a proper T–S fuzzy model on behalf of the original nonlinear plant
- Successful design of feasible robust position controller based on this T–S fuzzy model in the presence of parameters uncertainties as well as tool and motor disturbances
- Successful development of transient responses and disturbance attenuation of position tracking
- Successful robustness of the designed system ensuring that all closed-loop performance specifications are satisfied in the presence of unavoidable model uncertainty when the parameters in the system dynamic are varied in a wide range
- Successful design of controller in the event that the control signal (motor torque) does not exceed the allowable limit ± 20 Nm for the system even with a wide range of system uncertainties
- Successful superiority of proposed strategy in comparison with former design procedures

The paper is organized as follows. The proposed model and problem statement are described in Section 2. In Section 3, the design of robust H_2/H_∞ tracking controller is proposed. Simulation results of the closed-loop system with the proposed controller are presented in Section 4 and finally the paper is concluded in Section 5.

2. Model Description of ABB manipulator IRB6600

2.1 *Nonlinear mathematical model*

The most common type of industrial manipulators has six serially mounted links which are controlled by electrical motors and gears. A photograph of the ABB manipulator IRB6600 which shows its axes is presented in figure 1 (Moberg *et al* 2009; Wernholt & Gunnarsson 2006). The ABB-IRB6600 is a solid industrial manipulator and gear transmission in each axis possesses elasticity. A manipulator can be described as a nonlinear multivariable dynamical system having the six motor currents as the inputs, and the six measurable motor angles as outputs. For simplicity only the first axis of a horizontally mounted manipulator will be considered here. The remaining axes are positioned in a fixed configuration. In this way the influence of the nonlinear rigid body dynamics associated with the change of configuration (operating point) as well as gravity, centripetal, and coriolis torques can be neglected. Moreover, the remaining axes are positioned to minimize the couplings to the first axis. In this way, the control problem concerning the first axis can be approximated by an SISO control problem (Moberg *et al* 2009; Moberg 2007). The dynamics of the first axis of the robot includes both the actuator and the arm structure. The simulation model to be used is a four-mass model having nonlinear gear elasticity (Moberg *et al* 2009). This model is illustrated in figure 2. Hence, the manipulator dynamics can be described by the set of equations (Moberg *et al* 2009):

$$\begin{aligned}
J_m\ddot{q}_m &= u_m + w - f_m\dot{q}_m - k_1(q_m - q_{a_1}) - d_1(\dot{q}_m - \dot{q}_{a_1}) \\
J_{a_1}\ddot{q}_{a_1} &= -f_{a_1}\dot{q}_{a_1} + k_1(q_m - q_{a_1}) + d_1(\dot{q}_m - \dot{q}_{a_1}) - k_2(q_{a_1} - q_{a_2}) - d_2(\dot{q}_{a_1} - \dot{q}_{a_2}) \\
J_{a_2}\ddot{q}_{a_2} &= -f_{a_2}\dot{q}_{a_2} + k_2(q_{a_1} - q_{a_2}) + d_2(\dot{q}_{a_1} - \dot{q}_{a_2}) - k_3(q_{a_2} - q_{a_3}) - d_3(\dot{q}_{a_2} - \dot{q}_{a_3}) \\
J_{a_3}\ddot{q}_{a_3} &= \nu - f_{a_3}\dot{q}_{a_3} + k_3(q_{a_2} - q_{a_3}) + d_3(\dot{q}_{a_2} - \dot{q}_{a_3})
\end{aligned}$$

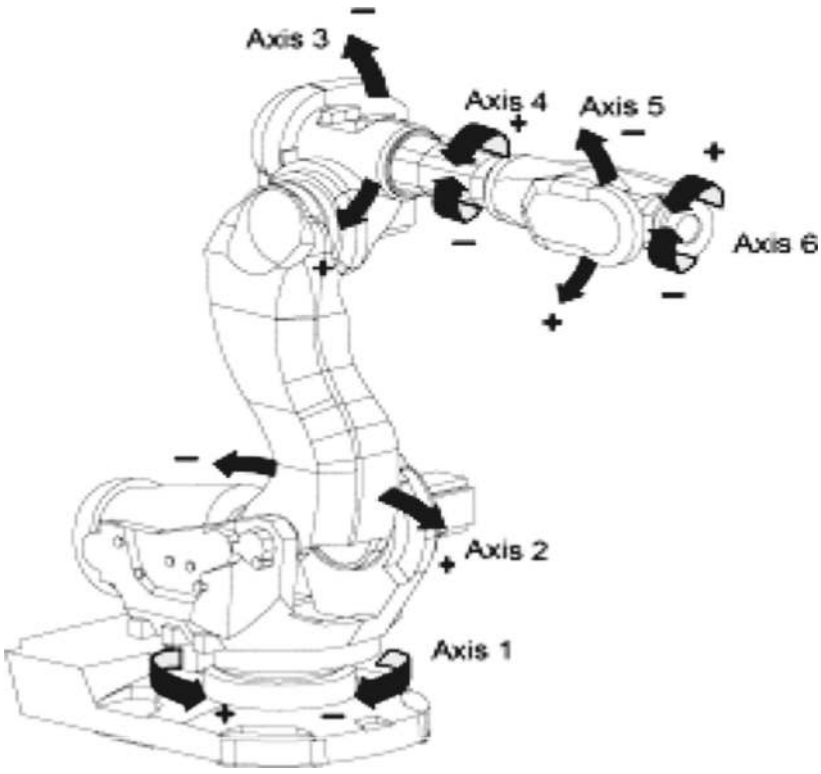

Figure 1. The ABB manipulator IRB6600.

The rotating masses are connected via spring-damper pairs. The first spring-damper pair, corresponding to the gear, has both the linear damping d_1 and the nonlinear elasticity k_1 While according to figure 2, elasticity of the first spring has nonlinear behavior, the part $k_1(q_m - q_{a_1})$ in (1) is replaced with a nonlinear function of the deflection $q_{\mathrm{m}} - q_{\mathrm{a1}}$, i.e., the entitled spring torque τ_{gear}. The modified version of Eq. (1) can be presented as

$$\begin{aligned}
J_m\ddot{q}_m &= u_m + w - f_m\dot{q}_m - \tau_{gear} - d_1(\dot{q}_m - \dot{q}_{a_1}) \\
J_{a_1}\ddot{q}_{a_1} &= -f_{a_1}\dot{q}_{a_1} + \tau_{gear} + d_1(\dot{q}_m - \dot{q}_{a_1}) - k_2(q_{a_1} - q_{a_2}) - d_2(\dot{q}_{a_1} - \dot{q}_{a_2}) \\
J_{a_2}\ddot{q}_{a_2} &= -f_{a_2}\dot{q}_{a_2} + k_2(q_{a_1} - q_{a_2}) + d_2(\dot{q}_{a_1} - \dot{q}_{a_2}) - k_3(q_{a_2} - q_{a_3}) - d_3(\dot{q}_{a_2} - \dot{q}_{a_3}) \\
J_{a_3}\ddot{q}_{a_3} &= v - f_{a_3}\dot{q}_{a_3} + k_3(q_{a_2} - q_{a_3}) + d_3(\dot{q}_{a_2} - \dot{q}_{a_3})
\end{aligned} \tag{1}$$

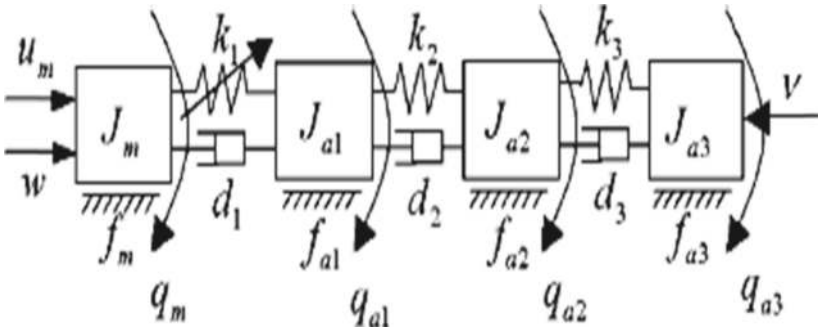

Figure 2. Model of manipulator.

A typical relationship between deflection and spring torques is illustrated in figure 3 (Moberg *et al* 2009). The second and third spring-damper pairs are both assumed to be linear and represented by d_2, k_2, d_3 and k_3. The moment of inertia of the arm is here split-up into the three components J_{a1}, J_{a2}, and J_{a3}. The moment of inertia of the motor is J_m. The parameters f_m, f_{a1}, f_{a2}, and f_{a3} represent viscous friction in the motor and the arm structure, respectively. The motor torque u_m, which is the manipulated input of the system, is limited to ± 20 Nm. The disturbance torque acting on the motor and tool is denoted by w and v, respectively. Angle of motor shaft is q_m The variables q_{a1}, q_{a2} and q_{a3} are arm angles of the three masses, and together they define the position of the tool. Although the angles in this model are expressed on the high-speed side of the gear, one must divide the model angles by the gear-ratio in order to get the real arm angles. For small variations around a given working point, the tool position, which is the controlled variable, can be calculated as Moberg *et al* (2009)

$$Z = \frac{l_1 q_{a_1} + l_2 q_{a_2} + l_3 q_{a_3}}{n}, \tag{2}$$

where n is the gear-ratio and l_1, l_2, l_3 are distances between the (fictive) masses and the tool.

2.2 *Proposed T-S fuzzy model*

In this section, a suitable function is first computed such that it exactly matches to the nonlinear curve torque-deflection in the specified domain shown in figure 3. The replaced function is given by

$$\tau_{gear} = 7500(q_m - q_{a1})^3 + 10(q_m - q_{a1}) \tag{3}$$

Using (3) in (1), the quasi-linear system of the nonlinear model can be expressed as

$$\dot{\underline{x}} = A\underline{x} + B_w W + B_v v + B_u u$$

$$A = \begin{bmatrix} 0 & 0 & 0 & 0 & 1 & 0 & 0 & 0 \\ 0 & 0 & 0 & 0 & 0 & 1 & 0 & 0 \\ 0 & 0 & 0 & 0 & 0 & 0 & 1 & 0 \\ 0 & 0 & 0 & 0 & 0 & 0 & 0 & 1 \\ -\frac{(7500R_1+10)}{J_m} & \frac{(7500R_2+10)}{J_m} & 0 & 0 & \frac{(f_m+d_1)}{J_m} & \frac{d_1}{J_m} & 0 & 0 \\ \frac{(7500R_1+10)}{J_{a_1}} & -\frac{(k_2+7500R_2+10)}{J_{a_1}} & \frac{k_2}{J_{a1}} & 0 & \frac{d_1}{J_{a_1}} & -\frac{(d_1+d_2+f_{a_1})}{J_{a_1}} & \frac{d_2}{J_{a_1}} & 0 \\ 0 & \frac{k_2}{J_{a_2}} & -\frac{(k_2+k_3)}{J_{a2}} & \frac{k_3}{J_{a2}} & 0 & \frac{d_2}{J_{a2}} & -\frac{(d_2+d_3+f_{a2})}{J_{a2}} & \frac{d_3}{J_{a2}} \\ 0 & 0 & \frac{k_3}{J_{a3}} & -\frac{k_3}{J_{a3}} & 0 & 0 & \frac{d_3}{J_{a3}} & -\frac{(d_3+f_a)}{J_{a3}} \end{bmatrix}$$

$$\begin{aligned} B_w &= \begin{bmatrix} 0 & 0 & 0 & 0 & \frac{1}{J_m} & 0 & 0 & 0 \end{bmatrix}^T \\ B_v &= \begin{bmatrix} 0 & 0 & 0 & 0 & 0 & 0 & 0 & \frac{1}{J_{a1}} \end{bmatrix}^T \\ B_u &= \begin{bmatrix} 0 & 0 & 0 & 0 & \frac{1}{J_m} & 0 & 0 & 0 \end{bmatrix}^T \end{aligned} \tag{4}$$

where $\underline{x}$ and R_1, R_2 are states vector and nonlinearity terms, respectively.

$$\begin{aligned} \underline{x} &= \begin{bmatrix} q_m & q_{a1} & q_{a2} & q_{a3} & \dot{q}_m & \dot{q}_{a1} & \dot{q}_{a2} & \dot{q}_{a3} \end{bmatrix}^T \\ R_1 &= {q_m}^2 + 3{q_{a1}}^2 \\ R_2 &= 3{q_m}^2 + {q_{a1}}^2. \end{aligned} \tag{5}$$

In view of the set of matrices (4), R_1 and R_2 appear only in matrix A. since the nonlinear system (1) is an affine model accordingly, R_1 and R_2 cannot be present at B_u, B_v and B_w. In

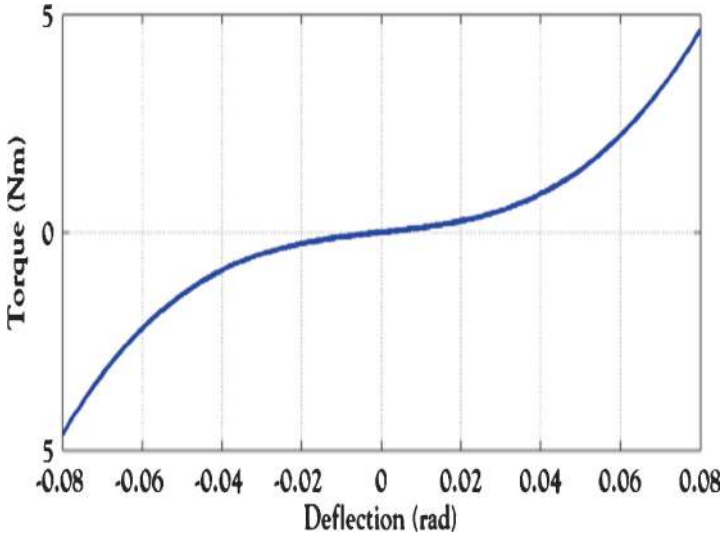

Figure 3. Nonlinear gear elasticity: Torque as function of deflection.

other words, matrix A is only influenced by the nonlinearity term R_1 and R_2. In this model, all of viscous frictions are supposed to differ from their nominal values. In the second part of this section, a T–S fuzzy model is proposed for the quasi-linear system (4). The T–S fuzzy dynamic model is described by fuzzy IF–THEN rules, which represent local linear input–output relations of nonlinear systems (Chen & Wu 2010; Wai & Yang 2008; Azimi *et al* 2012b, 2013a; Hua *et al* 2009; Zheng *et al* 2004; Assawinchaichote *et al* 2006). The fuzzy dynamic model is proposed by Takagi and Sugeno. The i$^{\text{th}}$ rule of T–S fuzzy dynamic model with parametric uncertainties can be described as follows:

$$\begin{aligned} &\textit{IF } R_1(t) \textit{ is } M_{i1} \textit{ and...and } R_p(t) \textit{ is } M_{ip} \textit{ THEN} \\ \dot{x}(t) &= [[A_i + \Delta A_i]x(t) + [B_{1i} + \Delta B_{1i}]w(t) + [B_{2i} + \Delta B_{2i}]u(t)], \qquad x(0) = 0 \\ z_\infty(t) &= [[C_{1i} + \Delta C_{1i}]x(t) + [D_{11i} + \Delta D_{11i}]w(t) + [D_{12i} + \Delta D_{12i}]u(t)] \\ z_2(t) &= [[C_{2i} + \Delta C_{2i}]x(t) + [D_{21i} + \Delta D_{21i}]w(t) + [D_{22i} + \Delta D_{22i}]u(t)] \\ i &= 1, 2...r \end{aligned} \tag{6}$$

where M_{ip} is the fuzzy set, r is the number of IF-THEN Rules and $R_1(t) \rightarrow R_p(t)$ are the premise variables, $x(t) \in R^n$ is the state vector, $u(t) \in R^m$ is the control input vector, $w(t) \in R^q$ is the disturbance input vector $w(t) = \begin{bmatrix} w \\ v \end{bmatrix}$. The matrices: ΔA_{i}, $\Delta B_{1\text{i}}$, $\Delta B_{2\text{i}}$, $\Delta C_{1\text{i}}$, $\Delta C_{2\text{i}}$, $\Delta D_{12\text{i}}$, $\Delta D_{21\text{i}}$, $\Delta D_{11\text{i}}$ and $\Delta D_{22\text{i}}$ represent the uncertainties in system (6). According to the local linearization approach (6), the local linear models for the system (4) are obtained in view of the aforementioned uncertainties (f_{m}, f_{a1}, f_{a2}, and f_{a3}). The overall fuzzy model can be represented given below.

$$\begin{aligned} \dot{x}(t) &= \sum_{i=1}^{r} \mu_i(\varphi(t))[[A_i + \Delta A_i]x(t) + [B_{1i} + \Delta B_{1i}]w(t) + [B_{2i} + \Delta B_2]u(t)], \\ &\quad x(0) = 0 \\ z_\infty(t) &= \sum_{i=1}^{r} \mu_i(R(t)[[C_{1i} + \Delta C_{1i}]x(t) + [D_{11i} + \Delta D_{11i}]w(t) + [D_{12i} + \Delta D_{12i}]u(t)]) \\ z_2(t) &= \sum_{i=1}^{r} \mu_i(R(t))[[C_{2i} + \Delta C_{2i}]x(t) + [D_{21i} + \Delta D_{21i}]w(t) + [D_{22i} + \Delta D_{22i}]u(t)] \end{aligned} \tag{7}$$

where $R\,(\mathrm{t}) = [R_1\,(\mathrm{t}) \ldots R_\mathrm{p}\,(\mathrm{t})\,]$ and the weighting function is defined as

$$\mu_i(R(t)) = \frac{\bar{\omega}(R(t))}{\sum_{i=1}^{r} \bar{\omega}(R(t))}$$

with

$$\bar{\omega}(R(t)) = \prod_{k=1}^{p} M_{ik}(R_k(t)) \tag{8}$$

It should be further noted that

$$\bar{\omega}(R(t)) \geq 0,\ i = 1, 2, ..., r;\ \sum_{i=1}^{r} \bar{\omega}_i(R(t)) > 0$$
$$\mu_i(R(t)) \geq 0,\ i = 1, 2, ..., r;\ \sum_{i=1}^{r} \mu_i(R(t)) = 1$$

3. Design of robust H_2/H_∞ tracking controller

3.1 *The PDC concept*

The concept of the PDC is utilized to design a fuzzy state feedback controller (Zheng *et al* 2004; Assawinchaichote *et al* 2006; Azimi *et al* 2012b). In this subsection, we focus on the design of a local pole-placement state feedback controller for each linear subsystem (6)

$$\begin{aligned} &\textit{IF } R_1\,(t) \textit{ is } M_{i1} \textit{ and... and } R_p\,(t) \textit{ is } M_{ip} \textit{ THEN} \\ &u(t) \;=\; K_i x(t),\ \ i = 1, 2, ..., r \end{aligned} \tag{9}$$

where K_i (i= 1, 2, . . . , r) are the local controller gains. According to the PDC approach, the control law of the whole system is the weighted sum of the local feedback control of each subsystem that can be expressed by

$$u\,(t) = \sum_{j=1}^{r} \mu_j K_j x\,(t), \tag{10}$$

where the local $\mathrm{H_2/H_\infty}$ multi-objective state feedback controller gains K_j are determined by LMI-based design techniques in order to fulfill the design requirements. In the next subsection, the state feedback controllers for each linear subsystem will be designed based on the LMI framework.

3.2 *Multi-objective H_2/H_∞ methodology*

To get a feeling for the multi-objective $\mathrm{H_2/H_\infty}$ methodology, consider the general pattern loop of figure 4. In this structure, $P(s)$ is the generalized plant, $K(s)$ is the controller, u is the control signal, x is the state vector, w is the exogenous signal and z_2 and z_∞ are the main objective. In this subsection, a multi-objective state-feedback synthesis is described by an LMI framework (Gahinet *et al* 1995; Gu *et al* 2005; Patra *et al* 2008; Azimi *et al* 2012b). The main objectives of multi-objective controller are expressed as $\mathrm{H_\infty}$ performance (for tracking, disturbance rejection or robustness aspects), $\mathrm{H_2}$ performance (for LQG aspects), robust pole placement specifications (to ensure fast and well-damped transient responses, reasonable feedback gain, etc.). Denote $T_\infty(s)$ and $T_2(s)$ as the closed-loop transfer functions from w to z_∞ and z_2, respectively. The main goal is to design a state-feedback law $u = Kx$ such that:

- It maintains the RMS gain ($\mathrm{H_\infty}$ norm) of T_∞ below some prescribed value $\gamma_0 > 0$,
- It maintains the $\mathrm{H_2}$ norm of $\mathrm{T_2}$ (LQG cost) below some prescribed value $\nu_0 > 0$,

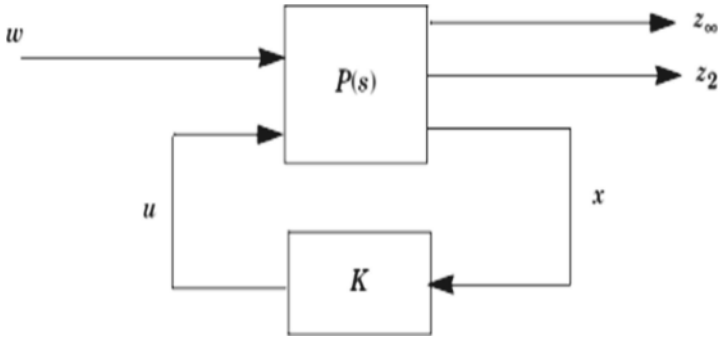

Figure 4. The control structure.

- It minimizes an H_2/H_∞ trade-off criterion of the form $\alpha \|T_\infty\|_\infty^2 + \beta \|T_2\|_2^2$
- It places the closed-loop poles in a prescribed LMI region.

Taken separately, three design objectives have the following LMI formulation for the state-space realization of each linear subsystem (6):

- **H_∞ performance:** the closed-loop RMS gain from w to z_∞ does not exceed γ if and only if there exists asymmetric matrix X_∞ such that

$$\begin{bmatrix} (A+B_2K)X_\infty + X_\infty(A+B_2K)^T & B_1 & X_\infty(C_1+D_{12}K)^T \\ B_1^T & -I & D_{11}^T \\ (C_1+D_{12}K)X_\infty & D_{11} & -\gamma^2 I \end{bmatrix} < 0$$
$$X_\infty > 0 \qquad (11)$$

- **H_2 performance:** the closed-loop H_2 norm of T_2 does not exceed ν if there exist two symmetric matrices X_2 and Q such that

$$\begin{bmatrix} Q & (C_2+D_{22}K)X_2 \\ X_2(C_2+D_{22}K)^T & X_2 \end{bmatrix} > 0$$
$$\begin{bmatrix} (A+B_2K)X_2 + X_2(A+B_2K)^T & B_1 \\ B_1^T & -I \end{bmatrix} < 0$$
$$Trace(Q) < \nu^2 \qquad (12)$$

- **Pole placement:** the closed-loop poles lie in the LMI Region D:

$$\begin{aligned} \mathcal{D} &= \left\{ z \in C : L + Mz + M^T\bar{z} < 0 \right\} \\ L &= ^TL^T = \left\{ \lambda_{ij} \right\}_{1 \le i,j \le m} \\ M &= \left\{ \mu_{ij} \right\}_{1 \le i,j \le m} \end{aligned}$$

if and only if there exists a symmetric matrix X_{pol} satisfies

$$\left[\lambda_{ij} X_{pol} + \mu_{ij}(A+B_2K)X_{pol} + \mu_{ij} X_{pol} + \mu_{ji} X_{pol}(A+B_2K)^T \right]_{1 \le i,j \le m} < 0$$
$$X_{pol} > 0$$

These three sets of conditions add up to an optimization problem with variables Q, K, X_∞, X_2 and X_{pol}. For tractability in the LMI framework, we seek a single Lyapunov matrix: $X := X_\infty = X_2 = X_{\text{pol}}$ that enforces all three objectives. With the change of variable $Y := KX$, this leads

to the following sub-optimal LMI formulation of our multi-objective state-feedback synthesis problem: Minimize $\alpha\gamma^2 + \beta$ Trace (Q) over Y, X, Q, and γ^2 satisfying (Wai & Yang 2008; Azimi *et al* 2012b)

$$\begin{bmatrix} AX + XA^T + B_2Y + Y^TB_2^T & B_1 & XC_1^T + Y^TD_{12}^T \\ B_1^T & -I & D_{11}^T \\ C_1X + D_{12}Y & D_{11} & -\gamma^2 I \end{bmatrix} < 0$$

$$\begin{bmatrix} Q & C_2X + D_{22}Y \\ XC_2^T + Y^TD_{22}^T & X \end{bmatrix} > 0$$

$$\left[\lambda_{ij} + \mu_{ij}\,(AX + B_2Y)\,X_{pol} + \mu_{ji}\left(XA^T + Y^TB_2^T\right)\right]_{1\le i,j\le m} < 0$$

$$Trace\,(Q) < \nu_0^2 \qquad \gamma^2 < \gamma_0^2 \tag{13}$$

Denoting the optimal solution by (X*, Y*, Q*, γ*) the corresponding state-feedback gain is given by K*=Y*(X*)$^{-1}$ and this gain guarantees the worst-case performance

$$\|T_\infty\|_\infty < \gamma^* \qquad \|T_2\|_2 < \sqrt{Trace(Q^*)}$$

3.3 *Proposed tracking controller*

In this research, the purpose is to design a suitable control which guarantees robust performance in the presence of parameter variations and disturbances. In this case, the control objective is position tracking of the tool (Z) when the tool moves along a certain desired path (Z_{ref}) as the designed controller can be robust in the presence of parameter variations and both the tool and motor disturbances. Also, the control signal (motor torque) does not exceed the allowable limit ±20 Nm for the system even with a wide range of system uncertainties. Therefore, to achieve an accurate tracking of tool position; the position tracking error (e_T) shall be minimized. Consequently, the main goal is to design a state-feedback controller such that: Maintains the RMS gain (H_∞ norm) of this e_T below some prescribed value $\gamma_0 > 0$. In order to do the minimization, an extra state is augmented to the quasi-linear system (4). The output of the integrator is considered as an extra state variable:

$$\begin{aligned} e_T &= Z_{ref} - Z \\ Z &= \frac{l_1q_{a_1} + l_2q_{a_2} + l_3q_{a_3}}{n} \end{aligned} \tag{14}$$

$$\begin{aligned} x_{aug} &= \int_0^t e_T\,(\delta)\,d\delta \\ \dot{x}_9 &= \dot{x}_{aug} = e_T. \end{aligned} \tag{15}$$

These goals are realized through constructing the objectives Z and the extra state in an appropriate control loop. Under the above considerations, the structure of the fuzzy robust control loop is proposed based on the structure depicted in figure 5.The quasi-linear system (4) given in figure 5 (a) is first approximated with some local linear models that each rule is represented by the T–S fuzzy approach. In order to obtain an accurate tracking of tool position, an extra state is then augmented to the T–S fuzzy model and the augmented plant is built. Separate controllers for each linear sub-plant are designed based on the LMI approach. After that the total system is obtained by using the weighted sum of the local linear systems and it is utilized on behalf of the original nonlinear system. According to the PDC approach, the control law of the whole system is the weighted sum of the local feedback control of all subsystems.

On the other hand, fuzzy weights (μ_i) are updated by using an FWOC component shown in figure 5(b). The blocks of the FWOC component are explained as follows:

- In the first block of this diagram the angle of motor shaft and the first mass values are measured in real time and nonlinear terms are built by these measurements.
- In the second block, the values of membership functions in current values of $R_1 R_2$ "nonlinearities" are calculated.
- In the thirdblock, new fuzzy weighting are calculated and they are sent to the main cotrol structure.

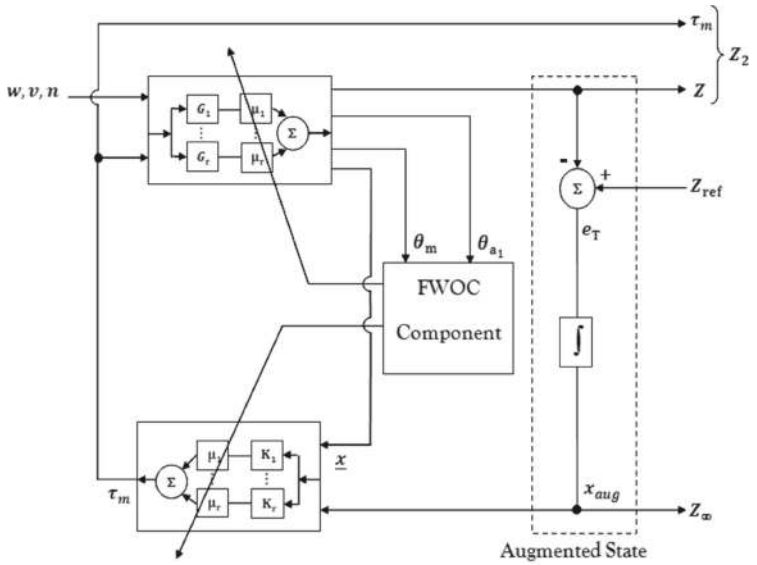

Figure 5. (a) The fuzzy robust control loop structure. (b) FOWC component.

Finally, by using the whole system and the global controller, a tracking loop (figure 5(a)) is applied to the system in order to achieve desirable specifications such as tracking performance, bandwidth, disturbance rejection, and robustness for the closed-loop system. More details of the procedure also are presented in Azimi *et al* (2013b).

4. Simulation results

In this section, we show the effectiveness of the proposed method by performing some simulation studies over three sets of an ABB flexible manipulator IRB6600 system. These sets are symbolized by M_{nom}, M_1, M_2, in the event that the set M_{nom} is indeed the nominal model and the sets M_1, M_2 introduce small and large variations in the physical parameters (min and max uncertainty of the system), respectively. The parameters of this manipulator are shown in table 1 (Moberg *et al* 2009). In this case, viscous frictions in the motor and the arm structure (f_m, f_{a1}, f_{a2}, and f_{a3}) are varied between $\pm 50\%$ (Moberg *et al* 2009; Moberg 2007). As a matter of fact, an industrial robot is influenced by various types of torque disturbances. They consist of torque disturbances acting on the motor and on the tool according to figure 6 and it is a combination of steps, pulses, and sweeping sinusoids (chirps) (Moberg *et al* 2009). In the quasi-linear system of flexible manipulator (4), the numbers of nonlinear terms $R_1 R_2$ are 2. According to the manipulator characteristics and the territory of the system operating points, we should calculate the minimum and maximum values of R_1 and R_2 as

$$R_i(t) = f\left(q_m(t), q_{a_1}(t)\right) \text{ and } q_m q_{a_1} \in [-\pi, \pi]$$

With regard to the above limitations, the membership functions can be taken as depicted in figure 7.

In the first step, the system (4) is represented by a T–S fuzzy model using the fuzzy rules given in (6). For this design problem, the rules r_1–r_4 are constructed for the T–S fuzzy model and referring to (4)–(6) the four linear subsystems are then calculated. In the second step, by using

Table 1. Nominal parameter values of manipulator.

Parameter	Value
J_m(kg.m^2)	0.005
J_{a_1}(kg.m^2)	0.002
J_{a_2}(kg.m^2)	0.02
J_{a_3}(kg.m^2)	0.02
k_2(Nm/rad)	110
k_3(Nm/rad)	80
d_1(Nm.s/rad)	0.08
d_2(Nm.s/rad)	0.06
d_3(Nm.s/rad)	0.08
f_m(Nm.s/rad)	0.006
f_{a_1}(Nm.s/rad)	0.001
f_{a_2}(Nm.s/rad)	0.001
f_{a_3}(Nm.s/rad)	0.001
l_1(mm)	20
l_2(mm)	600
l_3(mm)	1530
n	220

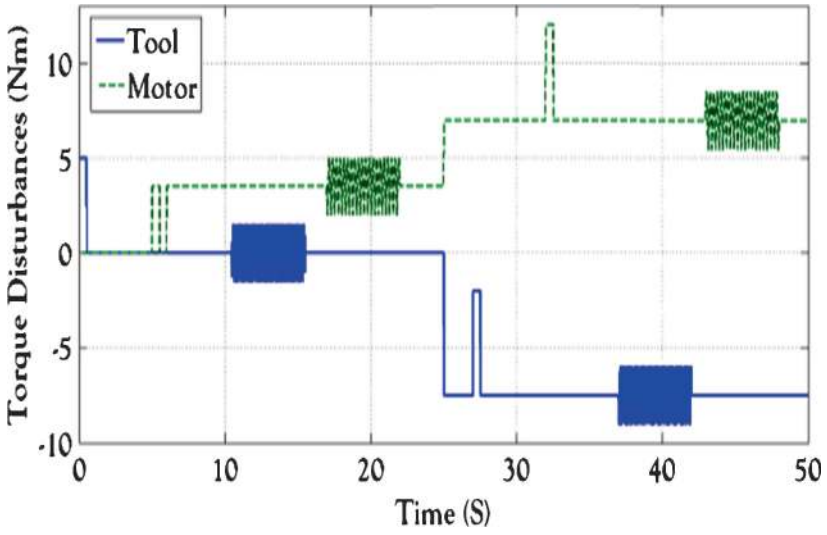

Figure 6. Torque disturbances on motor and tool.

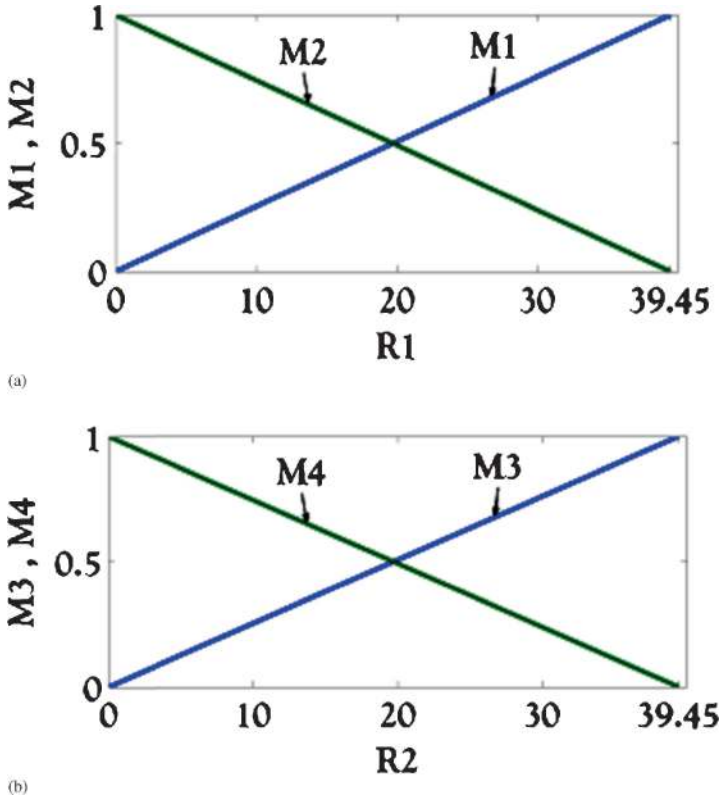

Figure 7. The membership functions for (a) $M_1(R_1)$ and $M_2(R_1)$, (b) $M_3(R_2)$ and $M_4(R_2)$.

the LMI formulations fully presented in subsection 3.2, we can calculate the local controllers for each linear subsystem. In order to design state-space feedback gains (K_i) for each subsystem, the following steps are done:

(1) Specify the LMI region D, in order to place the closed-loop poles in this region (pole placement) and also to guarantee some minimum decay rate and closed-loop damping. The aforementioned region is shown in figure 8, as the intersection of the half-plane $x < -5.5$ and of the sector centered at the origin with an inner angle

$$\theta = 2\pi/3(\mathcal{D} : x < -5.5 \text{ and } \theta = 2\pi/3).$$

(2) Choose a four-entry vector specifying the H_2/H_∞ cost function $(\alpha \|T_\infty\|_\infty^2 + \beta \|T_2\|_2^2)$: $[\gamma_0 \nu_0 \alpha \beta] = [0011]$.
(3) Minimize H_2/H_∞ cost function subject to the above-mentioned pole placement constraint using (11)–(12)–(13).

Finally, the overall fuzzy system is obtained by using a weighted average defuzzifer (WAD) and also the control law of the whole system is designed by using the PDC approach.

In practical applications, the states of the system are often not readily available; however, in this research according to the concept of the T–S fuzzy approach, states of the original nonlinear system are estimated by a separation principle (6) and alternatively, state feedback controller is employed based on these estimated states. In accordance with this point, an LMI-based fuzzy control is investigated using state feedback. Indeed, in this research an indirect robust controller is designed unlike the controller was directly hired in Azimi *et al* (2012b). Figure 9 compares states of the proposed T–S fuzzy model in comparison with the nonlinear system, where the dashed lines denote the estimated state variables $\underline{\hat{x}}(t)$ by the T–S fuzzy model and solid lines indicate states of the original nonlinear system $\underline{x}(t)$ in (1). Accordingly, design of a T–S fuzzy model is required to satisfy $\underline{\hat{x}}(t) \rightarrow \underline{x}(t)$ and this condition guarantees that the steady-state errors between $\underline{\hat{x}}(t)$ and $\underline{x}(t)$ converges to 0. As it is evident in this figure, the proposed T–S fuzzy model estimates states of the nonlinear benchmark model (1) without any steady-state error for

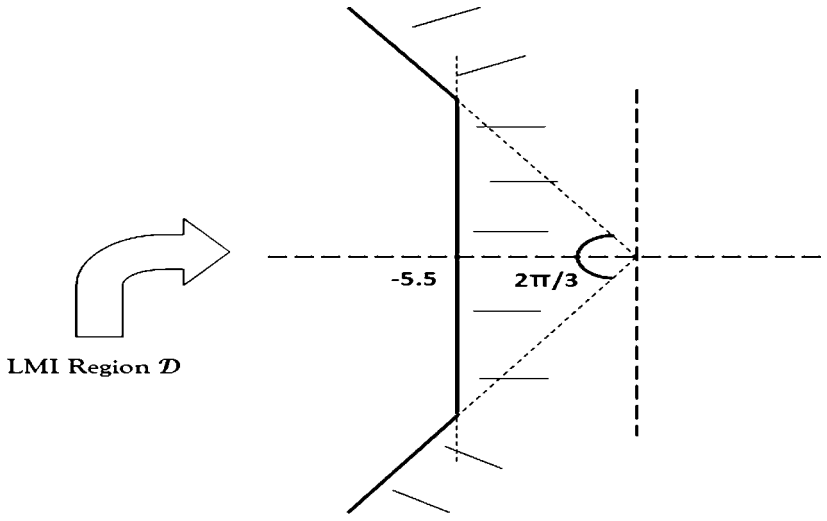

Figure 8. Pole placement region.

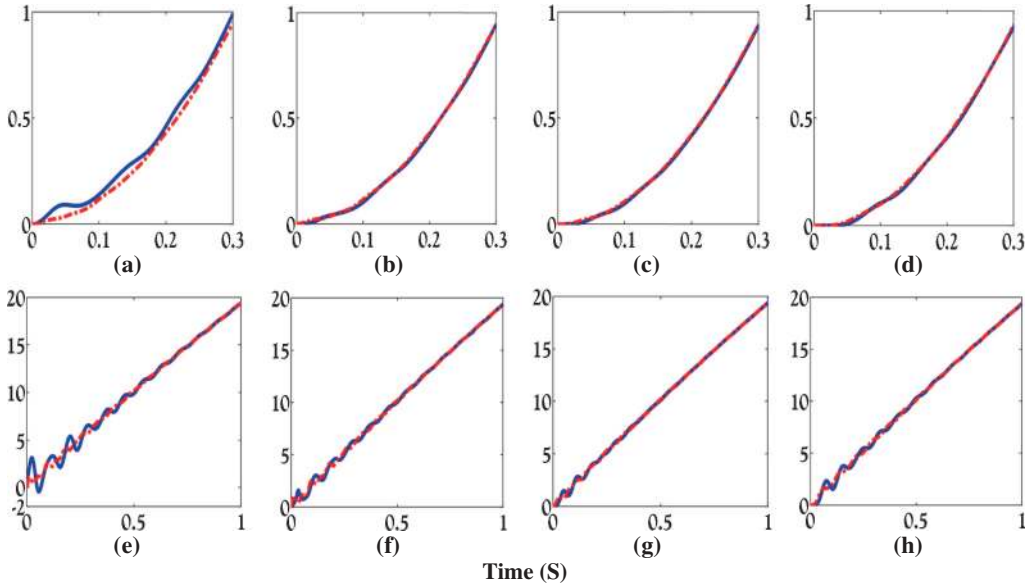

Figure 9. States of the proposed model $\hat{\underline{x}}(t)$ (dashed) and the nonlinear benchmark model $\underline{x}(t)$ (solid). (a) Angle of motor shaft q_m. (b) Arm angle of the first mass q_{a_1}. (c) Arm angle of the second mass q_{a_2}. (d) Arm angle of the third mass q_{a_3}. (e) Velocity of motor shaft $\dot{q}_m$. (f) Velocity of the first mass $\dot{q}_{a_1}$. (g) Velocity of the first mass $\dot{q}_{a_2}$. (h) Velocity of the first mass $\dot{q}_{a_3}$.

the range $x_1,\ x_2 \in [-\pi, \pi]$, which means that the fuzzy model can represent the original system in the pre-specified domains with a suitable approximation. Consequently, a complete T–S fuzzy model proposed can represent the nonlinear system in the region $[-\pi, \pi] \times [-\pi, \pi]$ on the $x_1 - x_2(q_{\mathrm{m}} - q_{\mathrm{a1}})$ space for various operating points. Figures 10 and 11 demonstrate that how the tool position (control objective) and the manipulated input (motor torque) of the nominal system ($\mathrm{M_{nom}}$) are influenced by the motor and tool disturbances (figure 6) as the proposed controller is used. The notations on figures 10 and 11 are described as follows:

- Peak-to-peak errors of the tool position curve (figure 10) are denoted by $e_1 - e_8$, where e_1, e_3, e_5, e_7 are created by the tool disturbance and e_2, e_4, e_6, e_8 are generated by motor disturbance.
- Settling times of the control objective (tool position) on figure 10 are symbolized by $T_{\mathrm{s}}^1 - T_{\mathrm{s}}^4$
- Maximum and adjusted rms values and torque "noise" (peak-to-peak) of input signal on figure 11 are represented by T_{MAX}, T_{RMS} and T_{NOISE} respectively.

Figure 12(a) and (b) shows motor torque and tracking of tool position to a certain command against motor and tool disturbances that are shown in figure 6, with regard to the proposed method. These figures illustrate the torque and position responses for all of the aforementioned parameter sets of system ($\mathrm{M_{nom}}$, $\mathrm{M_1}$ and $\mathrm{M_2}$), when the viscous friction in the motor and the arm structure (f_{m}, f_{a1}, f_{a2}, and f_{a3}) parameters are varied between $\pm 50\%$. It is clear that the system has good robustness when the parameters in the system dynamics are varied in a wide range.

As can be easily observed, the proposed method has good disturbance attenuation. According to figures 10 and 12(b), the proposed controller has the appropriate values of settling times ($T_{\mathrm{s}}^{\mathrm{i}}$), rise times, tool position tracking errors and peak-to-peak errors of the tool position (e_{i}). On the other hand, referring to figures 11 and 12(a), input signal is limited to ± 20 Nm and it has

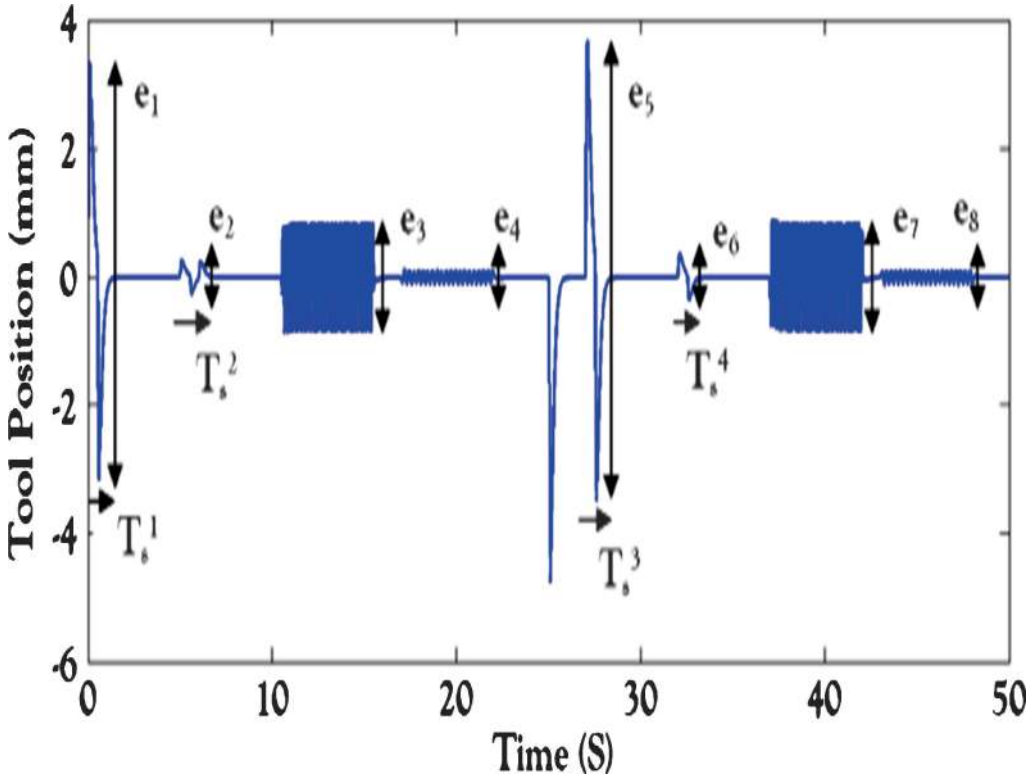

Figure 10. Tool position of manipulator.

satisfactory values of maximum and noise torque (T_{MAX}, T_{NOISE}). Compared with the paper presented in Azimi *et al* (2013b), in this research some cost functions will be expressed to make an accurate assessment of this work. Three cost functions V_{nom}, V_1, V_2 are described for three sets of flexible manipulator system, $\mathrm{M_{nom}}$, $\mathrm{M_1}$, $\mathrm{M_2}$ respectively, and they are given by Moberg *et al* (2009) and Moberg (2007):

$$\begin{aligned} V_{nom} &= \sum_{i=1}^{15} \alpha_i \{e_i\}_{on\ Mnom} \\ V_1 &= \sum_{i=1}^{15} \alpha_i \{\max(e_i)\}_{on\ M1} \\ V_2 &= \sum_{i=1}^{15} \alpha_i \{\max(e_i)\}_{on\ M2} \end{aligned} \tag{16}$$

where $e_1, \ldots, e_8$ have been defined before; $e_9, \ldots, e_{12}$ are $T_{\mathrm{s}}^1, \ldots, T_{\mathrm{s}}^4$; e_{13}, e_{14}, e_{15} represent T_{MAX}, T_{rms}, T_{NOISE}, respectively. Here the proposed fuzzy robust controller is used for all of the sets $\mathrm{M_{nom}}$, $\mathrm{M_1}$, $\mathrm{M_2}$. The adjusted RMS value of motor torque (input signal) $\mathrm{T_{RMS}}$ for all of these sets can be defined in time domain as

$$T_{RMS} = \sqrt{\frac{1}{n} \sum_{n} (T_m - T_{adj})^2} \tag{17}$$

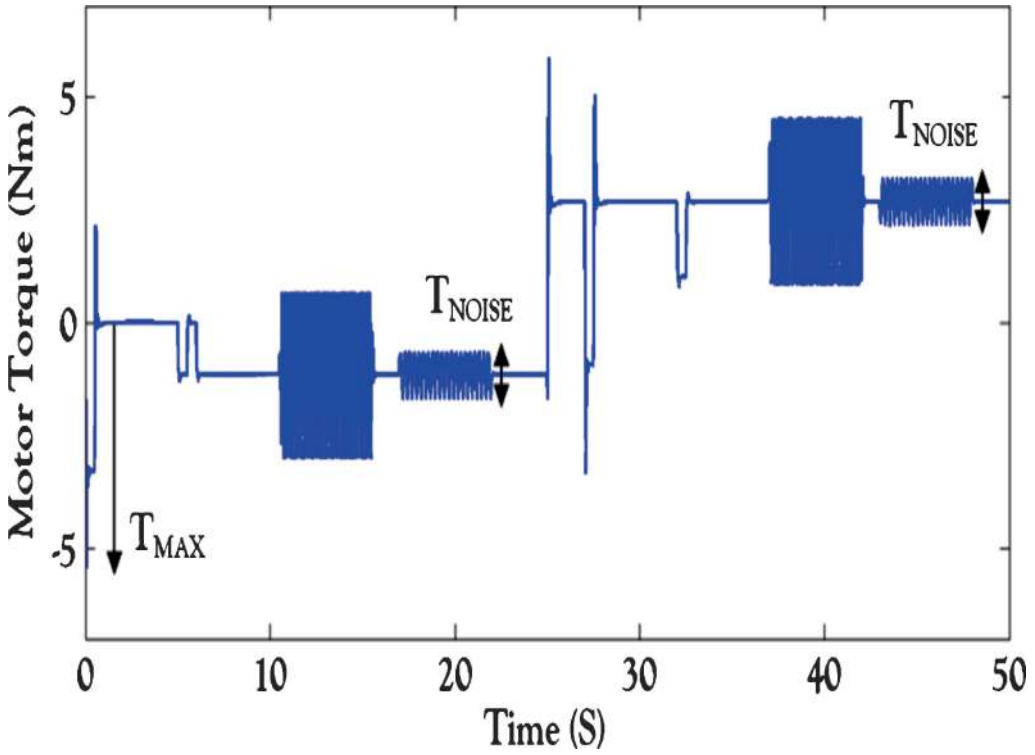

Figure 11. Motor torque of manipulator.

where T_m is the motor torque that has been already shown in figure 12(a), n is number of T_m samples and according to figure 12(a) T_{adj} are adjusted values of the torques that are presented for every set in table 2.

The whole cost function is symbolized by V to evaluate both the robustness and nominal performance, that is presented as

$$V = \beta_{nom} V_{nom} + \beta_1 V_1 + \beta_2 V_2 \tag{18}$$

Table 3 presents various classes of industrial coefficients α_i for sets M_{nom}, M_1, M_2 with the following definitions:

- **Class 1:** This class is determined in order to obtain a tradeoff between performance and robustness.
- **Class 2:** This class is defined to get control signal (motor torque) characteristic.
- **Class 3:** This class is utilized to gain tool position response trait (control objective) when torque disturbances just act on the tool.
- **Class4:** This class is used to achieve tool position response feature (control objective) when torque disturbances just act on the motor.
- **Class5:** This class is employed to evaluate peak-to-peak errors on tool position responses.
- **Class6:** This class is applied to assess settling times for tool position responses.
- **Class7:** This class is developed to obtain massive influence on design result.

Table 4 summarizes values of peak-to-peak errors (e_i), settling times (T_s^i), maximum, noise and adjusted RMS torques (T_{MAX}, T_{NOISE} and T_{RMS}) for all of the three sets that also have been

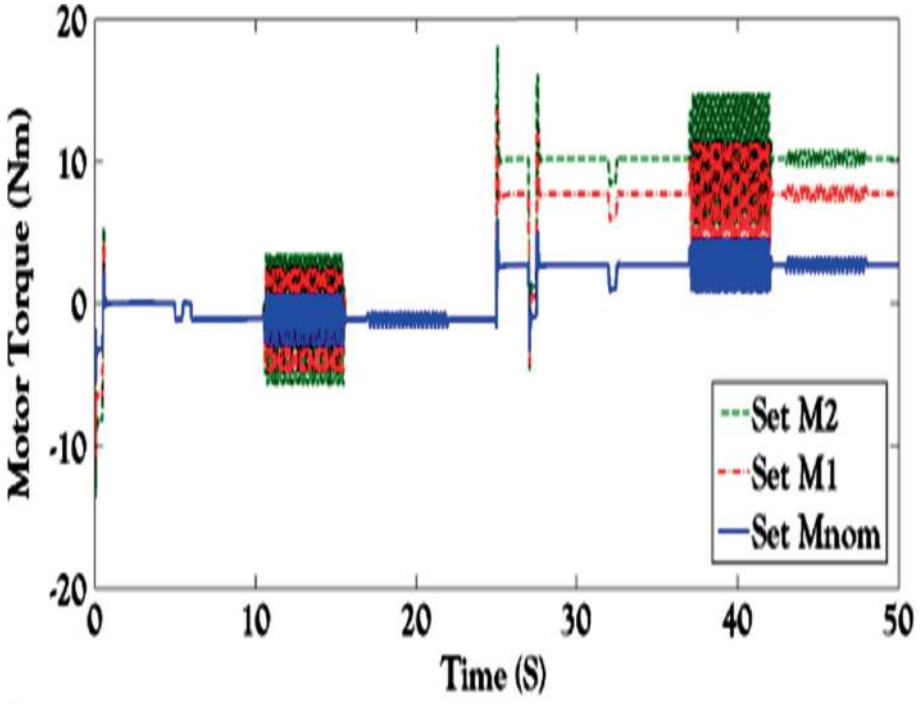

(a)

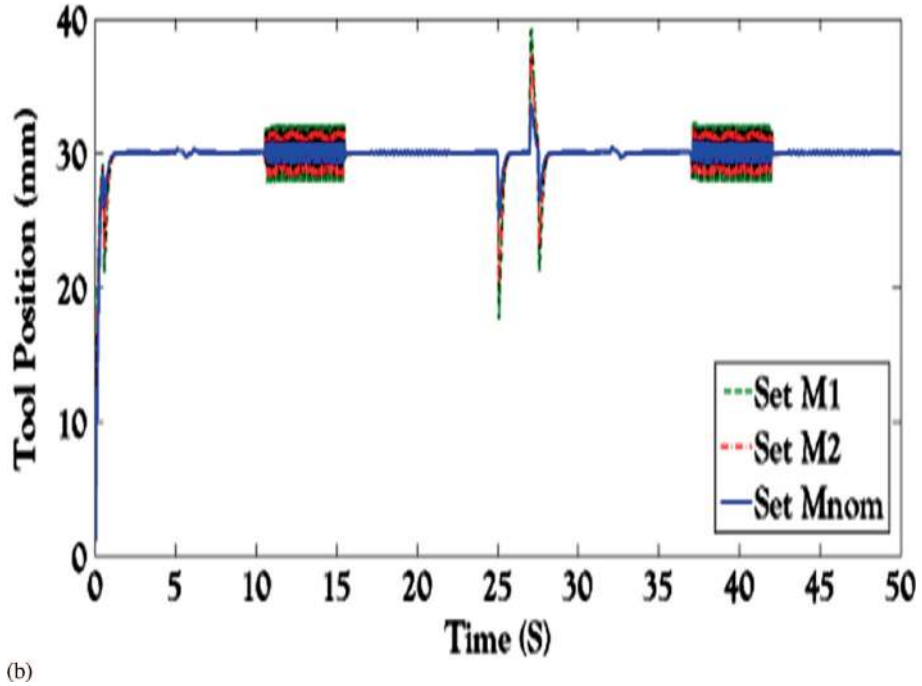

(b)

Figure 12. Torque and position responses of motor with viscous frictions uncertainties (a) Motor torque responses (b) tool position responses.

Table 2. Adjusted values of torques.

T_{adj} (Nm)	0≤time<5	5≤time<25	25≤time<50
T_{adj} for set M_{nom}	0	−1.2	2.7
T_{adj} for set M_1	0	−1.2	7.8
T_{adj} for set M_2	0	−1.2	10.3

already illustrated in figures 10, 11 and 12. This table is established when the proposed method is used.

Also, values of cost functions V_{nom}, V_1 and V_2, for each related set based on different classes of industrial coefficients (table 3) are presented in table 5. This table presents three cost function results based on three sets of an ABB flexible manipulator for the proposed approach over all kinds of classes.

In fact, numerical results of table 5 are fascinated by the aforementioned LMI region: $x < -5.5$ and $\theta = 2\pi/3$. Table 6 presents obtained values of cost functions V_{nom}, V_1 and V_2 in class1 for various LMI regions (pole placement region) over the position tracking response of the proposed method.

Table 6 proves that D1 is the optimal region among regions of this table, because the cost functions based on this region have the smallest values in comparison with other regions. In fact, values of peak-to-peak errors are increased when the inner angle θ is expanded, as well as settling timesare raised when the intersection of the half-plane x is reduced. Therefore, we have used design results based on the optimal LMI Region D1.To show the effectiveness of the proposed method, we compared the proposed controller with the following four solutions described in (Moberg *et al* 2009):

(A) A QFT controller proposed by P.-O. Gutman, Technion-Israel Institute of Technology, Haifa, Israel,

(B) A QFT controller of order 13 proposed by O. Roberto, Uppsala University, Uppsala, Sweden,

Table 3. Industrial coefficients values.

Coefficient	Class1	Class2	Class3	Class4	Class5	Class6	Class7
α_1	0.7	0	0.7	0	0.7	0	0.7
α_2	1.4	0	0	1.4	1.4	0	0
α_3	1.4	0	1.4	0	1.4	0	0
α_4	2.8	0	0	2.8	2.8	0	0
α_5	0.7	0	0.7	0	0.7	0	0.7
α_6	1.4	0	0	1.4	1.4	0	0
α_7	1.4	0	1.4	0	1.4	0	0
α_8	2.8	0	0	2.8	2.8	0	0
α_9	2.8	0	2.8	0	0	2.8	0
α_{10}	2.8	0	0	2.8	0	2.8	0
α_{11}	2.8	0	2.8	0	0	2.8	0
α_{12}	2.8	0	0	2.8	0	2.8	0
α_{13}	1.4	1.4	0	0	0	0	0
α_{14}	1.4	1.4	0	0	0	0	1.4
α_{15}	3.5	3.5	0	0	0	0	0

Table 4. Numerical results for proposed method.

Set	M_{nom}	M_1	M_2
$e_1(mm)$	6.50	13.10	16.25
$e_2(mm)$	0.51	0.50	0.53
$e_3(mm)$	1.70	3.41	4.20
$e_4(mm)$	0.23	0.22	0.24
$e_5(mm)$	7.23	14.43	17.93
$e_6(mm)$	0.74	0.74	0.78
$e_7(mm)$	1.73	3.41	4.31
$e_8(mm)$	0.24	0.23	0.23
$T_s^1(Nm)$	1.71	1.65	1.70
$T_s^2(Nm)$	2.21	2.20	2.20
$T_s^3(Nm)$	1.72	1.62	1.70
$T_s^4(Nm)$	1.80	1.75	1.81
$T_{NOISE}(Nm)$	1.00	1.01	1.08
$T_{MAX}(Nm)$	5.5	10.8	13.5
$T_{RMS}(Nm)$	0.92	2.4	2.72

(C) A polynomial controller proposed by F. Sikström and A.-K. Christiansson, University West, Sweden,

(D) A so-called linear sliding-mode controller proposed by W.-H. Zhu, Canadian Space Agency, Saint-Hubert, QC, Canada

The performance comparison for the set M_1 of the QFT controller in A, the QFT Controller of order 13 in B, the Polynomial Controller in C, Linear Sliding Mode Controller in D (Moberg *et al* 2009) and the proposed scheme is summarized in table 7.

Table 8 epitomize numerical results of the cost function V_1 referring to (16) for all methods based on various class of industrial coefficients.

Acording to this table, the value of the cost function V_1 in Classes 1, 4 and 5 for the proposed scheme is the least in comparison with the other methods. According to the records in class 4, better performances via quantities e_2, e_4, e_6, e_8, T_s^2 and T_s^4 are obtained through the proposed method. These quantities are peak-to-peak errors and setteling times of tool position when the torque disturbances act only on the motor. Although values of these quantities in the proposed method are lower than those of the other methods, the proposed controller can still give a better performance regarding both disturbance attenuation and transient time response in comparison with others when system is influenced by motor disturbances. Furthermore, based on the results in class 4, the proposed scheme has over 36, 37, 49 and 41% error reduction improvements in numerical results than the A, B, C and D systems, respectively when system is affected by both of motor and tool disturbances. Referring to class1 of this table, it can be observed that the proposed method outperforms remarkably other methods when a tradeoff between performance

Table 5. Cost functions V_{nom}, V_1 and V_2 for different classes.

Set	Class1	Class2	Class3	Class4	Class5	Class6	Class7
V_{nom}	50.6	12.3	24	14.3	17.4	20.8	17.3
V_1	77	24.9	35.5	14	29.4	20.2	34.3
V_2	89.7	29.9	45.3	14.4	38.9	20.7	42.8

Table 6. Performance of proposed method for various LMI regions.

	LMI region D			
	$\mathcal{D}1$	$\mathcal{D}2$	$\mathcal{D}3$	$\mathcal{D}4$
	$x < -5.5$	$x < -5.5$	$x < 0$	$x < 0$
Cost function	$\theta = 2\pi/3$	$\theta = 5\pi/6$	$\theta = 2\pi/3$	$\theta = 5\pi/6$
V_{nom}	50.6	53	53.6	57
V_1	77	79.5	81	85
V_2	89.7	91	92.2	96.9

Table 7. Performance comparisons for set M_1.

Proposed Algorithm	Control	A	B	C	D
e_1(mm)	13.10	8.22	8.57	9.75	9.11
e_2(mm)	0.50	2.56	2.43	3.41	3.22
e_3(mm)	3.41	5.39	5.56	5.34	5.28
e_4(mm)	0.22	1.58	1.74	2.12	1.77
e_5(mm)	14.43	7.78	8.22	9.37	8.64
e_6(mm)	0.74	2.82	2.82	4.02	3.68
e_7(mm)	3.41	4.88	5.13	4.20	4.59
e_8(mm)	0.23	1.40	1.56	1.90	1.57
T_s^1(Nm)	1.65	2.04	2.13	1.79	1.68
T_s^2(Nm)	2.20	1.25	1.47	1.52	1.05
T_s^3(Nm)	1.62	1.04	0.77	0.71	0.77
T_s^4(Nm)	1.75	0.95	0.55	0.69	0.71
T_{NOISE}(Nm)	1.01	2.67	1.05	1.85	1.66
T_{MAX}(Nm)	10.8	12.1	12.0	11.0	11.3
T_{RMS}(Nm)	2.4	1.53	1.52	1.43	1.46

and robustness is concerned. Although V_1 for our method has evidently higher values in classess 2, 3, 6 and 7, values of classess 2 and 3 are indeed very close to the related values of other methods. Records of class 2 show that our scheme has the lowest values of the maximum and noise torques (T_{MAX}, T_{NOISE}) while the value of T_{RMS} is the highest in comparison with others. On the other hand, based on the class 3 results, the proposed system has the highest value of V_1 when torque disturbances act only on the tool; however, this value is so close to that of A, B, C and D systems.

In fact, the proposed approach can give smaller values of whole items in table 7 in comparison with other methods, except settling times $T_s^1 T_s^2$, T_s^3, adjusted rms value and both of e_1 and e_5. Therefore, according to the results given in table 8, the values of V_1 in classes 6 and 7 for

Table 8. Numerical results comparisons of cost function V_1.

Control algorithm	Class1	Class2	Class3	Class4	Class5	Class6	Class7
Proposed	77	24.9	35.5	14	29.4	20.2	34.3
A	82.5	26.1	33.7	22	40.9	14.8	28.2
B	80.8	23.6	34.9	22.2	43.32	13.8	28.6
C	84.8	23	33.6	27.8	48.3	13.2	28.8
D	80.5	23.4	33.2	23.9	45.2	11.8	28.3

Table 9. Comparisons of cost function V_{nom}, V_1 and V_2 for Class1.

Control algorithm	Cost function		
	V_{nom}	V_1	V_2
Proposed	50.6	77.0	89.7
A	64.6	82.5	82.6
B	58.8	80.8	84.2
C	64.8	84.8	84.1
D	62.0	80.5	81.6

the proposed method become the highest in comparison with other methods with regard to the setteling time and massive influence characteristics. Values of the cost function V_{nom}, V_1 and V_2 for the proposed method in comparison with other algorithms based on class1 are gathered in table 9.

According to the results listed in table 9 some differences can be revealed between the proposed scheme and the other schemes. In short, referring to this table, it can be easily seen that the proposed method has the smallest values of the cost function V_1 and V_{nom}, though the cost function V_2 in our method has the worst value. Table 10 presents total numerical results of five methods based on the generalized cost function V (18) for class1. In this table, comparison of cost function results for various coefficients β is classified.

According to this table, the proposed method has the least value of the generalized cost function V in all of different coefficient groups; however, numerical results of the generalized cost function V only for class1 and group 1 were represented in Ref. (Zouand *et al* 2010). In this group, the coefficient of V_2 (β_2) in cost function V is smaller than other coefficients. Therefore,the whole cost funtion V is infuenced by V_2 less than V_1 and V_{nom} and as a result they are more important than V_2. From table 10, we can conclude that the performance of the presented method by the tested controllers is quite well and in turn the proposed robust tracking controller gives a better transient response and a smaller tracking error norm than the other control methods

Table 10. Comparisons of total results.

Group	Coefficients	Control algorithm				
		Proposed	A	B	C	D
1	$\beta_{nom} = 0.6$ $\beta_1 = 1$ $\beta_2 = 0.3$	134.3	146.0	141.4	148.9	142.2
2	$\beta_{nom} = 1$ $\beta_1 = 1$ $\beta_2 = 1$	217.3	229.7	223.8	223.7	224.1
3	$\beta_{nom} = 0.3$ $\beta_1 = 1$ $\beta_2 = 0.6$	146	151.4	148.9	154.7	148
4	$\beta_{nom} = 1$ $\beta_1 = 0.5$ $\beta_2 = 0.5$	134	147.1	141.3	149.2	143
5	$\beta_{nom} = 0.5$ $\beta_1 = 1$ $\beta_2 = 1$	192	197.4	194.4	201.3	193.1

do. In addition, both the robustness and nominal performance of the proposed method presented by the generalized cost function V are better than those of the control methods A, B, C and D in all of groups. Furthermore, the execution time of proposed controller (normalized CPU time per unit simulation) is 50 ms, while increase of computing power makes complicated control concepts feasible to implement and performance, robustness and easy tuning are more important factors.

5. Conclusion

In this paper, a robust H_2/H_∞ controller has been designed for tool position tracking and disturbance attenuation of a nonlinear uncertain flexible manipulator. First to approximate uncertain nonlinear system, the T–S fuzzy technique was employed. Then, we have shown that the proposed fuzzy model can accurately represent the original system in the pre-specified domains. Next, an extra state (tracking error) was augmented to the T–S model in order to improve the accuracy of the tracking control. After that for each linear subsystem, a robust pole-placement state feedback controller was appropriately designed by the LMI technique. Finally, the PDC method was used to design the controller for the overall system. The total linear system was then obtained through the weighted sum of the local linear system. A FWOC component was employed to update the fuzzy weights in real time for different system operating points. The simulation results on the manipulator were shown that the proposed control approach has robustness, precise tracking and good disturbances attenuation against load torque disturbances and parameter variations. In addition, the superiority of the proposed control scheme was approved in compared with the QFT controller, the QFT Controller of order 13, a polynomial controller and the so-called linear sliding-mode controller methods. Tables 8, 9 and 10 summarized performance comparisons for set M_1 and total results of five different methods, respectively. The major achievements of this research are: (i) the proposed T–S fuzzy model accurately represent the original nonlinear system in the pre-specified domains, (ii) both the robustness and nominal performance in the proposed method that have been presented by the generalized cost function V, were better than the control methods A, B, C and D, (iii) the control signal (motor torque) did not exceed the allowable limit ± 20 Nm for the three defined sets even with a wide range of system uncertainties.

Acknowledgements

The authors wish to acknowledge the Referees and the Associate Editor for their constructive comments and helpful suggestions that have helped to improve the quality of this paper. Moreover we would like to express their sincere gratitude to StigMoberg at ABB AB—Robotics, for his valuable guidance.

Appendix

Quasi-linear affine system presentation

The detailed quasi-linear affine model of original manipulator dynamics in (1) is presented in appendix.

By substituting (3) into (1), one can obtain

$$\begin{aligned}
J_m\ddot{q}_m &= u_m+w-f_m\dot{q}_m-[7500(q_m-q_{a_1})^3+10(q_m-q_{a_1})]-d_1(\dot{q}_m-\dot{q}_{a_1}) \\
J_{a_1}\ddot{q}_{a_1} &= -f_{a_1}\dot{q}_{a_1}+[7500(q_m-q_{a_1})^3+10(q_m-q_{a_1})]+d_1(\dot{q}_m-\dot{q}_{a_1}) \\
&\quad -k_2(q_{a_1}-q_{a_2})-d_2(\dot{q}_{a_1}-\dot{q}_{a_2}) \\
J_{a_2}\ddot{q}_{a_2} &= -f_{a_2}\dot{q}_{a_2}+k_2(q_{a_1}-q_{a_2})+d_2(\dot{q}_{a_1}-\dot{q}_{a_2})-k_3(q_{a_2}-q_{a_3})-d_3(\dot{q}_{a_2}-\dot{q}_{a_3}) \\
J_{a_3}\ddot{q}_{a_3} &= v-f_{a_3}\dot{q}_{a_3}+k_3(q_{a_2}-q_{a_3})+d_3(\dot{q}_{a_2}-\dot{q}_{a_3})
\end{aligned} \tag{19}$$

By expanding above equations, it is concluded that

$$\begin{aligned}
J_m\ddot{q}_m &= -\left(7500q_m^3+22500q_mq_{a_1}^2+10q_m\right)+\left(7500q_{a_1}^3+22500q_{a_1}q_m^2+10q_{a_1}\right) \\
&\quad -(f_m\dot{q}_m+d_1\dot{q}_m)+d_1\dot{q}_{a_1}+w+u_m \\
J_{a_1}\ddot{q}_{a_1} &= \left(7500q_m^3+22500q_mq_{a_1}^2+10q_m\right)-\left(7500q_{a_1}^3+22500q_{a_1}q_m^2+10q_{a_1}+k_2q_{a_1}\right) \\
&\quad +k_2q_{a_2}+d_1\dot{q}_m-(f_{a_1}\dot{q}_{a_1}+d_1\dot{q}_{a_1}+d_2\dot{q}_{a_1})+d_2\dot{q}_{a_2} \\
J_{a_2}\ddot{q}_{a_2} &= -f_{a_2}\dot{q}_{a_2}+k_2(q_{a_1}-q_{a_2})+d_2(\dot{q}_{a_1}-\dot{q}_{a_2})-k_3(q_{a_2}-q_{a_3})-d_3(\dot{q}_{a_2}-\dot{q}_{a_3}) \\
J_{a_3}\ddot{q}_{a_3} &= v-f_{a_3}\dot{q}_{a_3}+k_3(q_{a_2}-q_{a_3})+d_3(\dot{q}_{a_2}-\dot{q}_{a_3})
\end{aligned} \tag{20}$$

By factorization of system states (5), it yields

$$\begin{aligned}
\ddot{q}_m &= -\left[\frac{7500\left(q_m^2+3q_{a_1}^2\right)+10}{J_m}\right]q_m+\left[\frac{7500\left(q_{a_1}^2+3q_m^2\right)+10}{J_m}\right]q_{a_1} \\
&\quad -\left[\frac{f_m+d_1}{J_m}\right]\dot{q}_m+d_1\dot{q}_{a_1}+w+u_m \\
\ddot{q}_{a_1} &= \left[\frac{7500\left(q_m^2+3q_{a_1}^2\right)+10}{J_{a_1}}\right]q_m-\left[\frac{7500\left(q_{a_1}^2+3q_m^2\right)+10+k_2}{J_{a_1}}\right]q_{a_1} \\
&\quad +\frac{k_2}{J_{a_1}}q_{a_2}++\frac{d_1}{J_{a_1}}\dot{q}_m-\left[\frac{f_{a_1}+d_1+d_2}{J_{a_1}}\right]\dot{q}_{a_1}+\frac{d_2}{J_{a_1}}\dot{q}_{a_2} \\
\ddot{q}_{a_2} &= \frac{k_2}{J_{a_2}}q_{a_1}-\frac{(k_2+k_3)}{J_{a_2}}q_{a_2}+\frac{k_3}{J_{a_2}}q_{a_3}+\frac{d_2}{J_{a_2}}\dot{q}_{a_1}-\frac{(d_2+d_3+f_{a_2})}{J_{a_2}}\dot{q}_{a_2}+\frac{d_3}{J_{a_2}}\dot{q}_{a_3} \\
\ddot{q}_{a_3} &= \frac{k_3}{J_{a_3}}q_{a_2}-\frac{k_3}{J_{a_3}}q_{a_3}+d_3\dot{q}_{a_2}-\frac{(d_3+f_{a_3})}{J_{a_3}}\dot{q}_{a_3}+v
\end{aligned} \tag{21}$$

States of system $\underline{x}$ and nonlinearity terms $R_1 R_2$ can be expressed as follows:

$$\begin{aligned}
\underline{x} &= [\, q_m \;\; q_{a_1} \;\; q_{a_2} \;\; q_{a_3} \;\; \dot{q}_m \;\; \dot{q}_{a_1} \;\; \dot{q}_{a_2} \;\; \dot{q}_{a_3} \,]^T \\
R_1 &= q_m^2 + 3q_{a_1}^2 = x_1^2 + 3x_2^2 \\
R_2 &= 3q_m^2 + q_{a_1}^2 = 3{x_1}^2 + x_2^2
\end{aligned} \tag{22}$$

According to (20) and (21) the state-space quasi-linear model can be concluded

$$\begin{aligned}
\dot{x}_1 &= x_5 \\
\dot{x}_2 &= x_6 \\
\dot{x}_3 &= x_7 \\
\dot{x}_4 &= x_8 \\
\dot{x}_5 &= -\left[\frac{7500R_1+10}{J_m}\right]x_1 + \left[\frac{7500R_2+10}{J_m}\right]x_2 - \left[\frac{f_m+d_1}{J_m}\right]x_5 + d_1 x_6 + w + u_m \\
\dot{x}_6 &= \left[\frac{7500R_1+10}{J_{a_1}}\right]x_1 - \left[\frac{7500R_2+10+k_2}{J_{a_1}}\right]x_2 + \frac{k_2}{J_{a_1}}x_3 + + \frac{d_1}{J_{a_1}}x_5 \\
&\quad - \left[\frac{f_{a_1}+d_1+d_2}{J_{a_1}}\right]x_6 + \frac{d_2}{J_{a_1}}x_7 \\
\dot{x}_7 &= \frac{k_2}{J_{a_2}}x_2 - \frac{(k_2+k_3)}{J_{a_2}}x_3 + \frac{k_3}{J_{a_2}}x_4 + \frac{d_2}{J_{a_2}}x_6 - \frac{(d_2+d_3+f_{a_2})}{J_{a_2}}x_7 + \frac{d_3}{J_{a_2}}x_8 \\
\dot{x}_8 &= \frac{k_3}{J_{a_3}}x_3 - \frac{k_3}{J_{a_3}}x_4 + d_3 x_7 - \frac{(d_3+f_{a_3})}{J_{a_3}}x_8 + v
\end{aligned} \tag{23}$$

Consequently, the matrices of system (22) can be represented as

$$\dot{\underline{x}} = A\underline{x} + B_w w + B_v v + B_u u$$

$$A = \begin{bmatrix}
0_{4*4} & & & & I_4 & & & \\
-\frac{(7500R_1+10)}{J_m} & \frac{(7500R_2+10)}{J_m} & 0 & 0 & -\frac{(f_m+d_1)}{J_m} & \frac{d_1}{J_m} & 0 & 0 \\
\frac{(7500R_1+10)}{J_{a_1}} & -\frac{(k_2+7500R_2+10)}{J_{a_1}} & \frac{k_2}{J_{a_1}} & 0 & \frac{d_1}{J_{a_1}} & -\frac{(d_1+d_2+f_{a_1})}{J_{a_1}} & \frac{d_2}{J_{a_1}} & 0 \\
0 & \frac{k_2}{J_{a_2}} & -\frac{(k_2+k_3)}{J_{a_2}} & \frac{k_3}{J_{a_2}} & 0 & \frac{d_2}{J_{a_2}} & -\frac{(d_2+d_3+f_{a_2})}{J_{a_2}} & \frac{d_3}{J_{a_2}} \\
0 & 0 & \frac{k_3}{J_{a_3}} & -\frac{k_3}{J_{a_3}} & 0 & 0 & \frac{d_3}{J_{a_3}} & -\frac{(d_3+f_{a_3})}{J_{a_3}}
\end{bmatrix}$$

$$B = [\, B_w \;\; B_v \;\; B_u \,] = \begin{bmatrix}
0 & 0 & 0 \\
0 & 0 & 0 \\
0 & 0 & 0 \\
0 & 0 & 0 \\
\frac{1}{J_m} & \frac{1}{J_m} & 0 \\
0 & 0 & 0 \\
0 & 0 & 0 \\
0 & 0 & \frac{1}{J_{a_1}}
\end{bmatrix} \tag{24}$$

Referring above matrices, nonlinearity terms R_1 and R_2 and also uncertain parameters f_m, f_{a_1}, f_{a_2} and f_{a_3} appear only in matrix A. Define an affine parameter-dependent system is defined as:

$$\begin{aligned}
&\begin{cases} E(\rho)\dot{x} = A(\rho)x + B_1(\rho)w + B_2(\rho)u \\ z_\infty = C_1(\rho)x + d_{11}(\rho)w + d_{12}(\rho)u \\ z_2 = C_2(\rho)x + d_{12}(\rho)w + d_{22}(\rho)u \end{cases} \\
S(\rho) &= S_0 + \rho_1 S_1 + \ldots + \rho_n S_n \\
&\begin{bmatrix} A(\rho)+jE(\rho) & B(\rho) \\ C(\rho) & D(\rho) \end{bmatrix} = \begin{bmatrix} A_0+jE_0 & B_0 \\ C_0 & D_0 \end{bmatrix} + \rho_1 \begin{bmatrix} A_{\rho_1}+jE_{\rho_1} & B_{\rho_1} \\ C_{\rho_1} & D_{\rho_1} \end{bmatrix} \\
&+ \ldots + \rho_n \begin{bmatrix} A_{\rho_n}+jE_{\rho_n} & B_{\rho_n} \\ C_{\rho_n} & D_{\rho_n} \end{bmatrix} \\
&B(\rho) = \begin{bmatrix} B_1(\rho) & B_2(\rho) \end{bmatrix}, C(\rho) = \begin{bmatrix} C_1(\rho) & C_2(\rho) \end{bmatrix}^T, D(\rho) = \begin{bmatrix} d_{11}(\rho) & d_{12}(\rho) \\ d_{12}(\rho) & d_{22}(\rho) \end{bmatrix} \qquad (25)
\end{aligned}$$

where $S_0, S_1, \ldots, S_n$ are given system matrices; A(.), B(.), C(.), D(.) and E(.) are fixed affine functions of some vector $\rho = (\rho_1, \ldots, \rho_n)$ The parameters p_i are uncertain parameters. In this paper, uncertain parameters are given by following vector:

$$\rho = (\rho_1, \rho_2, \rho_3, \rho_4) = (f_m f_{a_1} f_{a_2} f_{a_3}) \qquad (26)$$

As a result, according to definition of (24) and uncertain parameters of (25), the matrix A can be decomposed as

$$A(\rho) = A_0 + \rho_1 A_1 + \rho_2 A_2 + \rho_3 A_3 + \rho_4 A_4 = A_0 + f_m A_{f_m} + f_{a_1} A_{a_1} + f_{a_2} A_{a_2} + f_{a_3} A_{a_3}$$

$$A = \begin{bmatrix} 0_{4*4} & & & & I_4 & & & \\ -\frac{(7500R_1+10)}{J_m} & \frac{(7500R_2+10)}{J_m} & 0 & 0 & -\frac{d_1}{J_m} & \frac{d_1}{J_m} & 0 & 0 \\ \frac{(7500R_1+10)}{J_{a_1}} & -\frac{(k_2+7500R_2+10)}{J_{a_1}} & \frac{k_2}{J_{a_1}} & 0 & \frac{d_1}{J_{a_1}} & -\frac{(d_1+d_2)}{J_{a_1}} & \frac{d_2}{J_{a_1}} & 0 \\ 0 & \frac{k_2}{J_{a_2}} & -\frac{(k_2+k_3)}{J_{a_2}} & \frac{k_3}{J_{a_2}} & 0 & \frac{d_2}{J_{a_2}} & -\frac{(d_2+d_3)}{J_{a_2}} & \frac{d_3}{J_{a_2}} \\ 0 & 0 & \frac{k_3}{J_{a_3}} & -\frac{k_3}{J_{a_3}} & 0 & 0 & \frac{d_3}{J_{a_3}} & -\frac{d_3}{J_{a_3}} \end{bmatrix}$$

$$A_{f_m} = \begin{bmatrix} 0_{4*8} \\ 0\ 0\ 0\ 0\ -\frac{1}{J_m}\ 0\ 0\ 0 \\ 0_{3*8} \end{bmatrix}, \qquad A_{a_1} = \begin{bmatrix} 0_{5*8} \\ 0\ 0\ 0\ 0\ 0\ -\frac{1}{J_{a_1}}\ 0\ 0 \\ 0_{2*8} \end{bmatrix}$$

$$A_{a_2} = \begin{bmatrix} 0_{6*8} \\ 0\ 0\ 0\ 0\ 0\ 0\ -\frac{1}{J_{a_2}}\ 0 \\ 0_{1*8} \end{bmatrix}, \qquad A_{a_3} = \begin{bmatrix} 0_{7*8} \\ 0\ 0\ 0\ 0\ 0\ 0\ 0\ -\frac{1}{J_{a_3}} \end{bmatrix} \qquad (27)$$

This completes the subsection 2.2 (Proposed T-S fuzzy model) of section 2 (Model Description of ABB manipulator IRB6600).

References

Asemani M H and Majd V J 2013 A robust H∞ observer-based controller design for uncertain T–S fuzzy systems with unknown premise variables via LMI. *Fuzzy Sets Syst.* 212: 21–40

Assawinchaichote W, Sing Kiong Nguang and Peng Shi 2006 Fuzzy control and filter design for uncertain fuzzy systems. Springer-Verlag Berlin Heidelberg

Azimi V, Akhlaghi P and Kazimi M H 2011 Robust multi objective H2/H∞ control of nonlinear uncertain systems using multiple linear model and ANFIS. *Chinese Control and Decision Conference (CCDC)*, China, 2011

Azimi V, Fakharian A and Menhaj M B 2012a Robust mixed-sensitivity gain-scheduled H_8 tracking control of a nonlinear time-varying IPMSM via a T-S fuzzy model. *9th France-Japan & 7th Europe-Asia Congress on and Research and Education in Mechatronics REM)*, France

Azimi V, Fakharian A and Menhaj M B 2013a Position and current control of a permanent-magnet synchronous motor by using loop-shaping methodology: Blending of H_∞ mixed-sensitivity problem and T-S fuzzy model scheme. *J. Dyn. Syst. Meas. Control-Trans. ASME* 135(5): 051006-1–051006-11

Azimi V, Nekoui M A and Fakharian A 2012b Robust multi-objective H2/ H∞ tracking control based on T-S fuzzy model for a class of nonlinear uncertain drive systems. *Proc. Inst. Mech. Eng. I-J. Syst. Control Eng.* 226(8): 1107–1118

Azimi V, Nekoui M A and Fakharian A 2012c Speed and torque control of induction motor by using robust H_∞ mixed-sensitivity problem via T-S fuzzy model. *Iranian Conference on Electrical Engineering (ICEE)*, Iran, 2012

Azimi V, Menhaj M B and Fakharian A 2013b Robust $H_2/_8$ control for a robust manipulator fuzzy system. *13th Iranian Conference on Fuzzy Systems (IFSC)*, Iran, 2013

Chen B-S and Wu C-H 2010 Robust optimal reference-tracking design method for stochastic synthetic biology systems: T-S fuzzy approach. *Fuzzy Syst. IEEE Trans.* 18(6): 1144–1159

El-Mahallawy A A *et al* 2011 Robust flight control system design using H∞ loop-shaping and recessive trait crossover genetic algorithm. *Expert Syst. Appl.* 38(1): 169–174

Fakharian A and Azimi V 2012 Robust mixed-sensitivity H8 control for a class of MIMO uncertain nonlinear IPM synchronous motor via T-S fuzzy model, *Methods and Models in Automation and Robotics (MMAR),* Poland, 2012

Gahinet P, Nemirovski A, Laub A J and Chilali M 1995 *LMI control toolbox.* Math Works

Gu D-W, Petkov P Hr and Konstantinov M M 2005 *Robust control design with MATLAB.* Springer-Verlag London

Hu S, Zhang Y, Yin X and Du Z 2013 T–S fuzzy-model-based robust stabilization for a class of nonlinear discrete-time networked control systems. *Nonlinear Anal.: Hybrid Syst.* 8: 69–82

Hua Ch, Wang Q-G and Guan X 2009 Robust adaptive controller design for nonlinear time-delay systems via T-S fuzzy approach. *IEEE Trans. Fuzzy Syst.* 17(4): 901–910

Islam S and Liu X P 2011 Robust sliding mode control of robot manipulators. *IEEE Trans. Ind. Electronics* 58(6)

Kamal E, Aitouche A and Abbes D 2014 Robust fuzzy scheduler fault tolerant control of wind energy systems subject to sensor and actuator faults. *Int. J. Electr. Power Energy Syst.* 55: 402–419

Li T-H S *et al* 2008 Robust H_∞ fuzzy control for a class of uncertain discrete fuzzy bilinear systems. *IEEE Trans. Syst. Man Cybern. - B: Cybern.* 38(2): 510–527

Moberg S 2007 On modeling and control of flexible manipulators. *Thesis, Dept. Electric. Eng., Linkoping Univ.,* Sweden

Moberg S and Hanssen S 2007 A approach to feed forward control of flexible manipulators. In: *IEEE Int. Conf. Robotics Automation*, Roma, Italy, April 2007, pp. 10–14

Moberg S and Öhr J 2005 Robust control of a flexible manipulator arm: A benchmark problem. In: *16th IFAC World Congr.*, Prague, Czech Republic, July 2005

Moberg S and Öhr J 2008 Swedish open championships in robot control. *Open Championships*, Sweden

Moberg S, Öhr J and Gunnarsson S 2008 A benchmark problem for robust control of a multivariable nonlinear flexible manipulator. In: *17th IFAC World Congr.*, Seoul, South Korea, July 2008

Moberg S, Ohr J and Gunnarsson S 2009 A benchmark problem for robust feedback control of a flexible manipulator. *IEEE Trans. Control Syst. Technol.* 17(6): 1398–1405

Ohr J *et al* 2006 Identification of flexibility parameters of 6-axis industrial manipulator models. In: *Int. Conf. Noise Vibration Eng. (ISMA)*, Leuven, Belgium, Sept. 2006, pp. 3305–3314

Patra S, Sen S and Ray G 2008 Design of static H∞ loop shaping controller in four-block framework using LMI approach. *Automatica* 44(8): 2214–2220

Shayeghi H, Jalili A and Shayanfar H A 2008 A robust mixed H2/Hinf based LFC of a deregulated power system including SMES. *Energy Conversion Manag* 49(10): 2656–2668

Wai R-J and Yang Z-W 2008 Adaptive fuzzy neural network control design via a T-S fuzzy model for a robot manipulator including actuator dynamics. *Systems, Man, Cybern. B: Cybern. IEEE Trans.* 38(5): 1326–1346

Wai R-J, Huang Y-C, Yang Z-W and Shih C-Y 2010 Adaptive fuzzy-neural-network velocity sensorless control of robot manipulator position tracking. *IET Control Theory Appl.* 4(6): 1079–1093

Wernholt E and Gunnarsson S 2006 Detection and estimation of nonlinear distortions in industrial robots. In: *IEEE Instrumentation and Measurement Technology Conf.*, Sorrento, Italy, April 2006

Wu X, Wang Y and Dang X 2014 Robust adaptive sliding-mode control of condenser-cleaning mobile manipulator using fuzzy wavelet neural network. *Fuzzy Sets Syst.* 235: 62–82

Yang H, Li X, Liu Z and Zhao L 2014a Robust fuzzy-scheduling control for nonlinear systems subject to actuator saturation via delta operator approach. *Inf. Sci.* 272: 158–172

Yang H, Shi P, Li X and Li Z 2014b Fault-tolerant control for a class of T–S fuzzy systems via delta operator approach Original Research Article. *Signal Process* 98: 166–173

Yue D and Lam J 2004 Suboptimal robust mixed H_2/H_{inf} controller design for uncertain descriptor systems with distributed delays. *Comput. Math. Appl.* 47(6–7): 1041–1055

Zheng F, Wang Q-G and Lee T H 2004 Adaptive and robust controller design for uncertain nonlinear systems via fuzzy modeling approach. *IEEE Trans. Syst. Man Cybern. B: Cybern.* 34(1): 166–178

Zouand Y *et al* 2010 Neural network robust Hinf tracking control strategy of robot manipulators. *Appl. Math. Model.* 34(7): 1823–1838